Iran J Public Health, Vol. 52, No.5, May 2023, pp.1019-1030

Original Article

Identification of Lncrna-Mrna Networks in Hepg2 Cells upon *ATP7B* Knockout and Copper Accumulation

Yan Yan, Yin Xu, Lin Chen, Yongzhu Han, Renmin Yang, *Wenbin Hu

Affiliated Hospital of the Institute of Neurology, Anhui University of Chinese Medicine, Hefei, 230061, P.R. China

***Corresponding Author:** Email: hwb8012@163.com

(Received 15 Nov 2022; accepted 08 Jan 2023)

Abstract

Background: Hepatolenticular degeneration (HLD) is an inherited disorder caused by the mutation in the adenosine triphosphatase copper transporting β gene (*ATP7B*). W aimed to explore the genetic changes in HLD using bioinformatics analysis.

Methods: The study was conducted in Nepal, in 2019. The GSE107323 dataset was downloaded and the differentially expressed lncRNAs (DElncRNAs) as well as differentially expressed genes (DEGs) induced by *ATP7B* knockout (KO) and copper toxicity were clustered using Mfuzz clustering analysis. LncRNAs and genes with high coexpression (correlation coefficient > 0.9) and pathways involving the DEGs were used to construct the lncRNA-gene-pathway network.

Results: *ATP7B* KO and *ATP7B* KO + copper induced 51 overlapping DEGs and 687 overlapping DElncRNAs, respectively. Mfuzz analysis identified four clusters, including two clusters of consistently upregulated and downregulated DEGs/DElncRNAs. The lncRNA-gene-pathway network consisted of 13 DElncRNAs, 10 DEGs, and two pathways, including "hsa04630: Jak-STAT signaling pathway" and "hsa04920: Adipocytokine signaling pathway". Eight downregulated genes, including erythropoietin (*EPO*), insulin receptor substrate 1 (*IRS1*), and PPARG coactivator 1 alpha (*PPARGC1A*), and two upregulated genes (cardiotrophin-like cytokine factor 1 and cyclin D3) were involved in the two pathways. These genes were targeted by multiple lncRNAs, including *PCAT6* and *MALAT1*.

Conclusion: Collectively, the differentially expressed lncRNA-mRNA axes play crucial roles in HLD pathogenesis through mediating cell proliferation and inflammation. Moreover, the *EPO*, *IRS1*, or *PPARGC1A* genes were potent therapeutic targets for HLD.

Keywords: Hepatolenticular degeneration; Adenosine triphosphatase copper transporting β; Bioinformatics analysis; Copper accumulation

Introduction

Hepatolenticular degeneration (HLD) is an inherited and autosomal recessive disorder caused by the inherited mutations in the adenosine triphosphatase copper (Cu) transporting β gene (*ATP7B*) (1). *ATP7B* mutation impairs hepatic Cu transport and metabolism, leads to aberrant Cu accumulation and tissue damage of the liver, brain, cornea, and kidney (2-4). Hepatic dysfunc-

tion was the most common initial symptom in HLD patients (2, 5). The presymptomatic diagnosis of HLD is difficult due to the lack of diagnostic criteria and untreated symptomatic patients progress rapidly to death. The early diagnosis and the prevention of HLD progression are still urgent medical problems to be solved.

ATP7B is a Cu chaperone that mainly expresses in the hepatocytes (6). *ATP7B* mutations lead to Cu metabolic disorder by blocking the loading of Cu into the serum, the synthesis of the Cu–protein ceruloplasmin, and the transport of superfluous Cu into the bile. Accordingly, *ATP7B* mutation leads to Cu accumulation and toxicity in the target organs (5, 7). Hepatocytes from HLD patients and *ATP7B*$^{-/-}$ mice had increased autophagosomes (6). Besides, the knockout (KO) of *ATP7B* in HepG2 cells exposed to Cu significantly increased a cluster of autophagy-related genes (6). However, the exact molecular mechanisms induced by *ATP7B* mutation and Cu toxicity-induced organ damage are not clear.

We aimed to investigate the molecular mechanisms of HLD using a cellular model induced by *ATP7B* KO and Cu toxicity. The microarray dataset GSE107323, deposited by Polishchuk et al. (6) was downloaded. The differentially expressed lncRNAs (DElncRNAs) and differentially expressed genes (DEGs) induced by *ATP7B* KO and Cu toxicity would be identified to illustrate the lncRNA-mRNA regulatory mechanism that may be involved in HLD pathogenesis.

Materials and Methods

Microarray dataset

The microarray dataset GSE107323 (GPL18573, Illumina NextSeq 500, Homo sapiens) (6) was downloaded from the Gene Expression Omnibus (https://www.ncbi.nlm.nih.gov/) on May 20, 2020. GSE107323 contained 12 samples and the nine samples from untreated WT (n = 3), untreated *ATP7B* KO (n = 3), and Cu-treated *ATP7B* KO cells (n = 3) were downloaded and used for the bioinformatics analysis of this study.

Data processing

The data files (.txt format) were downloaded and preprocessed using the R3.4.1 Core (https://www.bioconductor.org/packages/devel/bioc/html/preprocessCore.html; version 1.44). Data were normalized using the quantiles methods. Then, the annotation of lncRNAs and protein-coding genes was performed in the HUGO Gene Nomenclature Committee (HGNC) database (https://www.genenames.org/).

Identification of DElncRNAs and DEGs

The DElncRNAs and DEGs induced by *ATP7B* KO with and without Cu treatment were identified using the edgeR package (http://www.bioconductor.org/packages/release/bioc/html/edgeR.html; version 3.28.1) (8). DElncRNAs and DEGs between the WT and *ATP7B* KO cells with and without Cu treatment were identified according to the criteria of false discovery rate < 0.05, $p < 0.05$, and $|\log_2(\text{fold change})| > 1$. The overlapping items induced by *ATP7B* KO with and without Cu were identified using the Venny diagram (version 2.1; https://bioinfogp.cnb.csic.es/tools/venny/index.html). Bilateral hierarchical clustering heatmap expression profiles of the overlapping items in samples were presented using the R pheatmap package (https://cran.r-project.org/package=pheatmap; version 1.0.8).

Functional enrichment analysis

The Database for Annotation, Visualization and Integrated Discovery (DAVID; https://david.ncifcrf.gov/; version 6.8) provides a comprehensive set of functional annotation tools for investigators to understand biological meaning behind a large list of genes. The Gene Ontology categories and Kyoto Encyclopedia of Genes and Genomes (KEGG) pathways significantly associated with DEGs were analyzed using the functional enrichment analysis in the DAVID database, with the criteria of $P < 0.05$ and gene count ≥ 2.

Mfuzz clustering analysis

The expression patterns of DElncRNAs and DEGs in HepG2 cell samples were clustered using the Mfuzz package (http://www.bioconductor.org/packages/release/bioc/html/Mfuzz.html; version 2.42.0) (9). Genes and lncRNAs that had similar expression profiles upon *ATP7B* KO with and without Cu toxicity were clustered together. The biological processes and KEGG pathways significantly associated with the DEGs in the same clusters were identified in DAVID when $p < 0.05$ and gene count ≥ 2.

Construction of the lncRNA-mRNA coexpression network

The coexpression relationships between the DEGs and lncRNAs in the same cluster were analyzed using the R cor.test (https://stat.ethz.ch/R-manual/R-devel/library/stats/html/cor.test.html; version R3.4.1). The Pearson correlation coefficients (r) between lncRNAs and genes were analyzed and coexpression pairs with $r > 0.9$ (positive correlation with high confidence) were retained and used to construct the lncRNA-mRNA coexpression network using the Cytoscape software (http://www.cytoscape.org/; version 3.8.0). Moreover, the biological processes and KEGG pathways associated with DEGs in the lncRNA-mRNA network were identified in DAVID with $P < 0.05$ and gene count ≥ 2.

Construction of the lncRNA-gene-pathway network

Pathways that might be related to HLD were identified from the Comparative Toxicogenomics Database (CTD, 2020 update; http://ctd.mdibl.org/) database using the keywords of "Hepatolenticular Degeneration" or "Wilson disease". The common pathways between HLD-related KEGG pathways in CTD and DAVID were retained and used for the construction of the lncRNA-gene-pathway network.

Results

Identification of DElncRNAs and DEGs

After matching against the HGNC database, 3455 lncRNAs and 12864 genes were annotated in the original data files of the dataset GSE107323. A total of 1478 (including 1385 DEGs and 93 DElncRNAs) and 2720 (including 2522 DEGs and 198 DElncRNAs) items were identified from the *ATP7B* KO HepG2 cells treated with and without Cu, respectively, as compared with the WT cells (Fig. 1A and B). The distinct expression patterns of the DEGs/DElncRNAs in HepG2 cells were shown by the hierarchical clustering heatmap (Fig. 1C and D).

Overlapping genes and functional enrichment analysis

The Venn diagram showed that there were 738 common DEGs and DElncRNAs between the two treatments, including 51 DElncRNAs and 687 DEGs (Fig. 2A and Table S1). Functional enrichment analysis showed that the common DEGs were associated with 22 biological processes, including "GO:0042592: homeostatic process" and "GO:0055082: cellular chemical homeostasis", and 12 KEGG pathways, including "hsa03320: PPAR signaling pathway", "hsa04630: Jak-STAT signaling pathway", and "hsa04920: Adipocytokine signaling pathway" (Table S2).

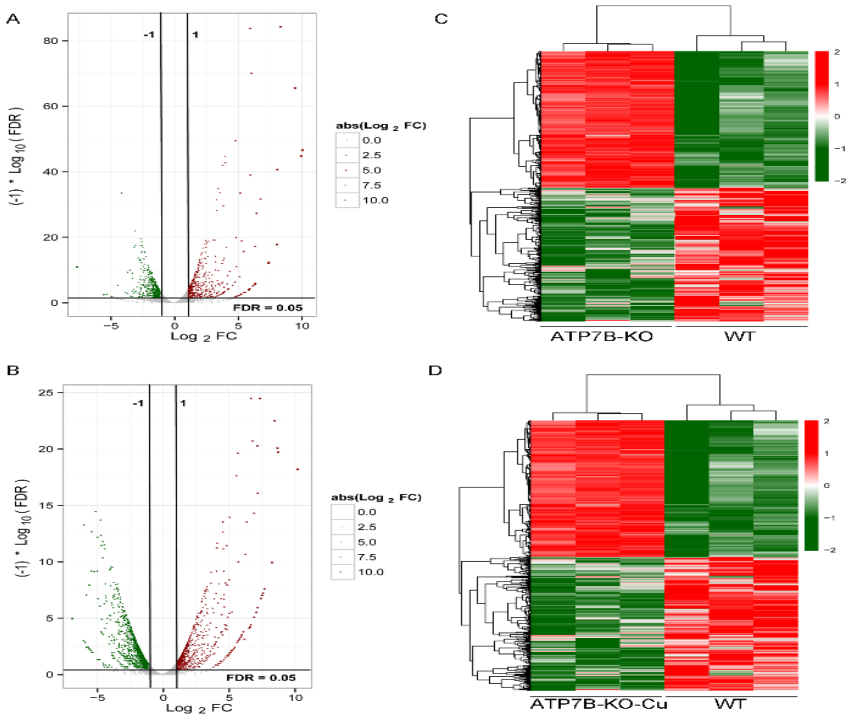

Fig. 1: The differentially expressed lncRNAs and genes in HepG2 cells in response to *ATP7B* knockout (KO) and copper accumulation. A and B, the Volcano plots of the differentially expressed lncRNAs and genes in HepG2 cells upon *ATP7B* KO and *ATP7B* KO + Cu, respectively, compared with wild-type (WT) cells. FC, fold change. FDR, false discovery rate. Red for upregulation and green for downregulation. C and D, the hierarchical clustering heatmaps of the differentially expressed lncRNAs and genes in samples, respectively. Red and green colors note high and low expression, respectively

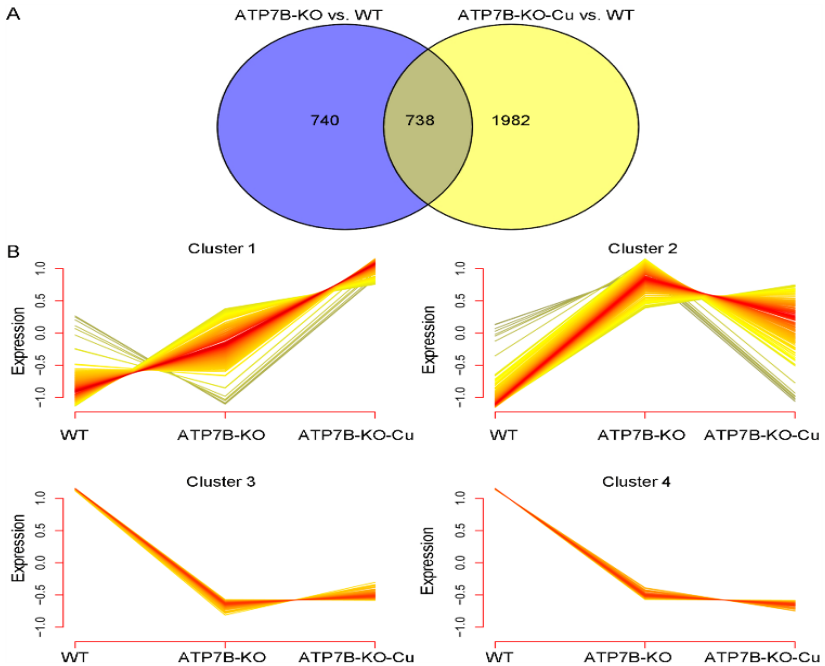

Fig. 2: Mfuzz clustering analysis of the differentially expressed genes and lncRNAs. A, the Venn diagram showing the number of differentially expressed lncRNAs and genes in HepG2 cells upon *ATP7B* knockout (KO) with and without Cu toxicity. B, four Mfuzz clusters of genes with different expression patterns on *ATP7B* KO and Cu toxicity. WT, wild-type

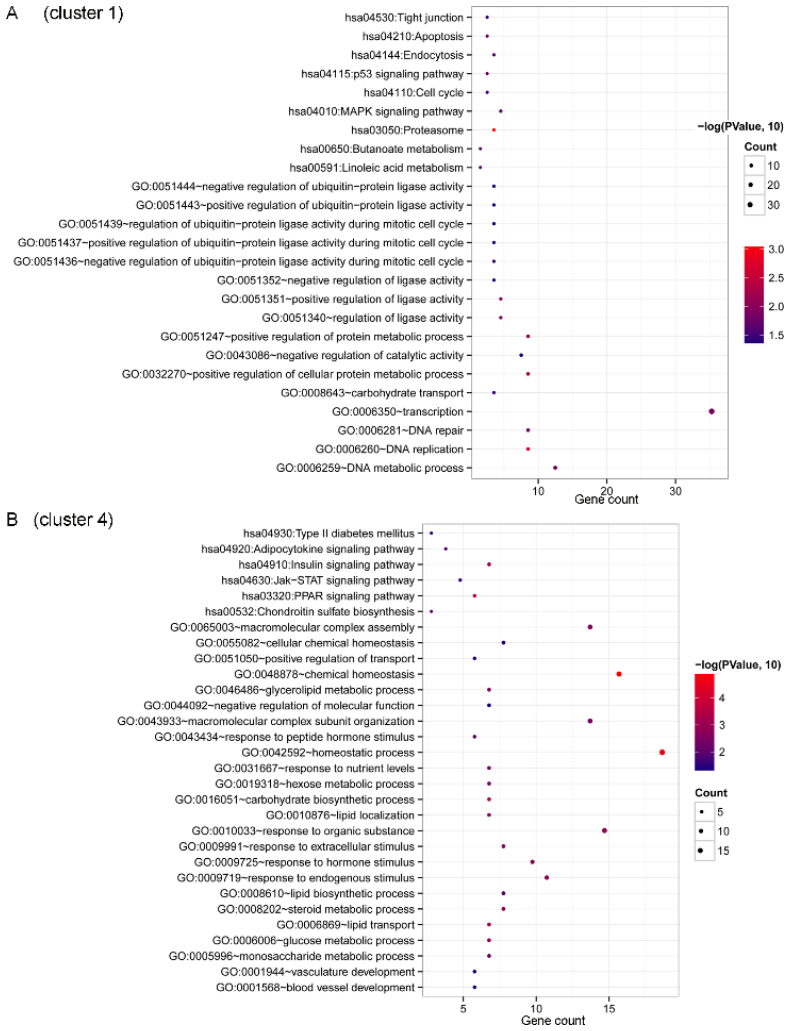

Fig. 3: Results of functional enrichment analysis for the differentially expressed genes in clusters 1 and 4. A and B, bubble diagrams showing the significantly enriched biological processes and pathways associated with the genes in clusters 1 and 4, respectively

Clustering of the genes/lncRNAs

Mfuzz clustering analysis showed that the 738 common DEGs/DElncRNAs were clustered into four gene clusters (Fig. 2B). Genes/lncRNAs in clusters 1 and 2 were generally upregulated upon *ATP7B* KO, and genes/lncRNAs in clusters 3 and 4 were downregulated, respectively. Besides, the combined treatment with Cu toxicity consistently elevated the expression levels of genes/lncRNAs in Cluster 1, and decreased the expression levels of genes/lncRNAs in Cluster 4.

Functional categories associated with genes in Clusters 1 and 4

Functional enrichment analysis showed that the Cluster 1 DEGs were associated with 16 biological processes (Fig. 3A), including "GO:0051247: positive regulation of protein metabolic process" and "GO:0006260: DNA replication", and nine KEGG pathways, including "hsa04115: p53 signaling pathway". The Cluster 4 DEGs were enriched with 24 biological processes (Fig. 3B), including "GO:0010033: response to organic substance" and "GO:0043933: macromolecular complex subunit organization", and six pathways, including "hsa03320: PPAR signaling pathway",

"hsa04630: Jak-STAT signaling pathway", and "hsa04920: Adipocytokine signaling pathway".

The lncRNA-mRNA coexpression networks of clusters 1 and 4

Correlation analysis identified 1070 lncRNA-mRNA coexpression pairs with r > 0.9 (Table S3). The lncRNA-mRNA regulatory networks of clusters 1 and 4 are shown in Fig. 4, inclusive of 23 DElncRNAs and 280 DEGs. Eighteen and five lncRNAs were included in the networks of clusters 1 and 4, respectively (Fig. 4A and B). LncRNAs including prostate cancer-associated lncRNA transcript 6 (*PCAT6*, cluster 4), DDN and PRKAG1 antisense RNA 1 (*DDN-AS1*, cluster 4), transducer of ERBB2, 1 antisense RNA 1 (*TOB1-AS1*, cluster 4), and afadin divergent transcript (*AFDN-DT*, cluster 4) interacted with 119, 116, 113, and 100 DEGs in the networks, respectively.

DEGs in the lncRNA-mRNA coexpression networks were associated with 19 biological processes, including "GO:0042592: homeostatic process" and "GO:0043933: macromolecular complex subunit organization", and six KEGG pathways, including "hsa03320: PPAR signaling pathway", "hsa04920: Adipocytokine signaling pathway", and "hsa04630: Jak-STAT signaling pathway" (Fig. 5 and Table 1).

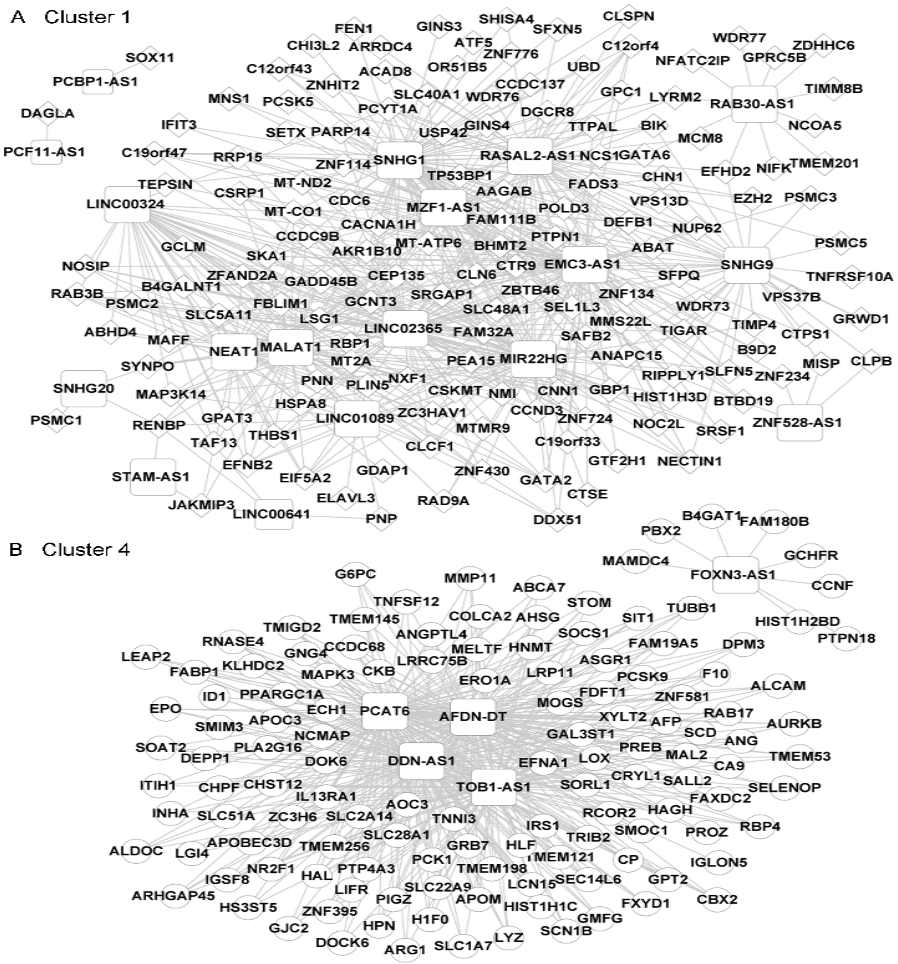

Fig. 4: The lncRNA-mRNA regulatory networks of the genes/lncRNAs in clusters 1 and 4, respectively. A and B, the lncRNA-mRNA regulatory network involving the differentially expressed genes/lncRNAs in cluster 1 and cluster 4, respectively. All the lncRNA-mRNA interaction pairs have high Pearson correlation coefficients (>0.9). LncRNAs are indicated by squares, and genes in clusters 1 and 4 are noted by diamonds (upregulation) and cycles (downregulation), respectively

Table 1: The pathways associated with the differentially expressed genes in the lncRNA-mRNA regulatory networks

Pathways	***Number***	***P-value***	***Genes (clusters)***
hsa03320:PPAR signaling pathway	6	3.900E-03	*SCD* (4), *APOC3* (4), *FABP1* (4), *SLC27A5* (4), *PCK1* (4), *ANGPTL4* (4)
hsa04910:Insulin signaling pathway	7	1.685E-02	*G6PC* (4), *SOCS1* (4), *MAPK3* (4), *PTPN1* (1), *PPARGC1A* (4), *IRS1* (4), *PCK1* (4)
hsa03050:Proteasome	4	3.474E-02	*PSMC5* (1), *PSMC3* (1), *PSMC2* (1), *PSMC1* (1)
hsa00532:Chondroitin sulfate biosynthesis	3	4.402E-02	*XYLT2* (4), *CHPF* (4), *CHST12* (4)
*hsa04920:Adipocytokine signaling pathway	4	4.828E-02	*G6PC* (4), *PPARGC1A* (4), *IRS1* (4), *PCK1* (4)
*hsa04630:Jak-STAT signaling pathway	6	4.884E-02	*CCND3* (1), *CLCF1* (1), *SOCS1* (4), *LIFR* (4), *IL13RA1* (4), *EPO* (4)

Two overlapped pathways in Comparative Toxicogenomics Database are noted by stars (*). The number in parentheses after gene symbol represents the cluster to which the gene belongs

The lncRNA-gene-pathway network

A total of 112 HLD-associated KEGG pathways were identified in the CTD database. Two pathways, including "hsa04920: Adipocytokine signaling pathway" and "hsa04630: Jak-STAT signaling pathway", were common to the pathways of DEGs in the lncRNA-mRNA coexpression networks. Four cluster 4 genes were included in the "hsa04920: Adipocytokine signaling pathway", and four cluster 4 genes and two cluster 1 genes were enriched with the "hsa04630: Jak-STAT signaling pathway" (Table 2). Accordingly, the lncRNA-gene-pathway network (Fig. 6), in which 10 DEGs, 13 DElncRNAs, and two pathways were included, was constructed. Genes erythropoietin (*EPO*), insulin receptor substrate 1 (*IRS1*), and PPARG coactivator 1 alpha (*PPARGC1A*) interacted with four lncRNAs, including *AFDN-DT*, *TOB1-*

Table 2: Drug-gene interaction pairs identified in the pharmacogenetics and pharmacogenomics knowledgebase

Gene Symbols	***Chemical ID***	***Chemical Name***	***Variation Name***	***Gene IDs***	***PMID***
EPO	PA450085	Irinotecan	rs1800734	PA134917440,PA240	30519050
EPO	PA451241	Ribavirin	rs1617640	PA27833	25227310
IRS1	PA449972	Imiquimod	rs2004640	PA29919	24223576
IRS1	PA449053	Clopidogrel	rs13431554	PA203	27005817
PPARGC1A	PA451241	Ribavirin	rs1801282	PA281	25072612
PPARGC1A	PA450395	Metformin	rs2970852	PA33558	24317794

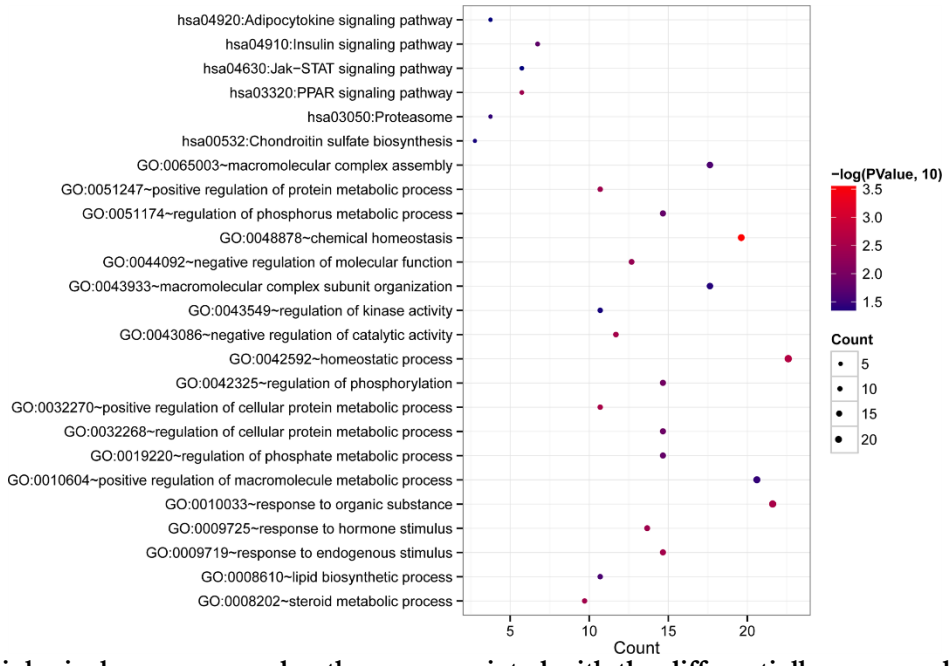

Fig. 5: The biological processes and pathways associated with the differentially expressed genes in the lncRNA-mRNA networks of clusters 1 and 4. Bubble diagrams showing the significantly enriched biological processes (n=16) and pathways (n=9) associated with genes in the lncRNA-mRNA networks of clusters 1 and 4

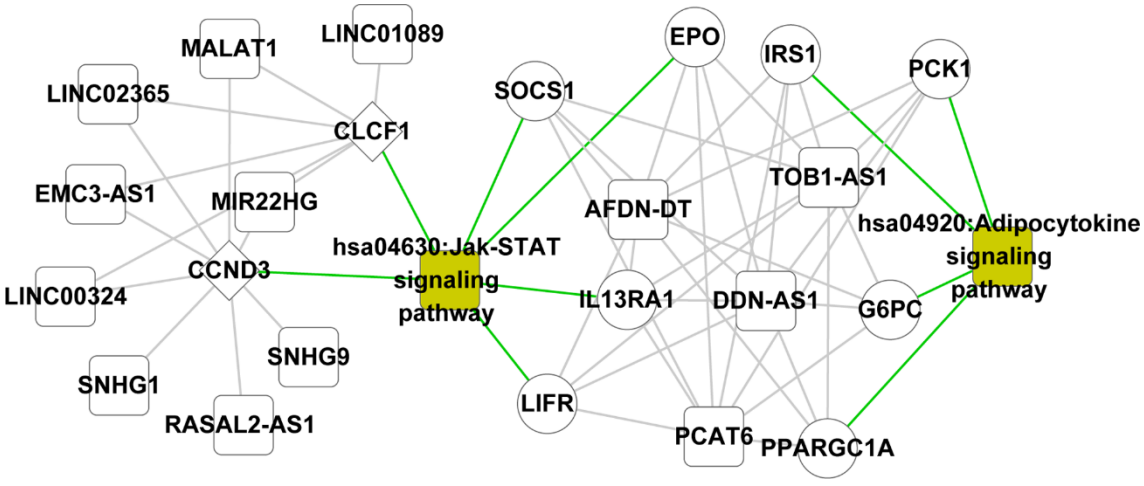

Fig. 6: The lncRNA-gene-pathway network. The final lncRNA-gene-pathway network consists of 13 lncRNAs (empty squares), 10 genes (cluster 1: diamonds, and cluster 4: circles), and two pathways (yellow squares). Involvement in pathways is shown by a green line

AS1, *DDN-AS1*, and *PCAT6*. The cardiotrophin-like cytokine factor 1 (*CLCF1*) and cyclin D3 (*CCND3*) genes were regulated by six and eight lncRNAs, respectively, including metastasis-associated lung adenocarcinoma transcript 1 (*MALAT1*), long intergenic non-protein coding RNA 00324 (*LINC00324*), and MIR22 host gene (*MIR22HG*). *IRS1* and *PPARGC1A* were involved in the "hsa04920: Adipocytokine signaling pathway". Two cluster 1 genes (*CLCF1* and *CCND3*) and *EPO* were enriched in the "hsa04630: Jak-STAT signaling pathway" (Fig. 6).

Discussion

Recent advances in the computational bioinformatics approaches are of great value in hunting disease genes, biomarkers, molecular mechanisms, and therapeutic targets (10, 11). This study identified the potential molecular mechanisms of HLD pathogenesis and development using bioinformatics. We found that *ATP7B* KO and Cu accumulation in HepG2 cells led to the differential expression of a large number of lncRNAs and genes. LncRNAs *MALAT1*, *LINC00324*, *MIR22HG*, and DEGs *CLCF1* and *CCND3* were upregulated in HepG2 cells upon *ATP7B* KO and Cu toxicity treatments. Those genes were associated with several signaling pathways, including "hsa04920: Adipocytokine signaling pathway" and "hsa04630: Jak-STAT signaling pathway", and were also involved in the homeostatic process. These molecules may be the genetic characteristics of HLD.

ATP7B KO in HepG2 cells exposed to Cu significantly increased the expression of 103 autophagy-related genes, including autophagy-related gene 7 (*ATG7*) and *ATG13* (6). However, the inhibition of autophagy accelerated Cu toxicity-induced cell death in *ATP7B* KO HepG2 cells (6). They deduced that autophagy protected *ATP7B* KO cells from Cu-induced cell death. Excessive Cu-induced oxidative stress and autophagy had been identified previously in chicken hepatocytes (12) and human cancer cells (13). We also found that the expression of *ATG3*, *ATG5*, and *ATG7* were downregulated in WT HepG2 cells by Cu accumulation and *ATP7B* KO, but not *ATP7B* KO plus Cu toxicity (data not shown). In addition, other autophagy-related genes, including the Fas-associated death domain protein gene and the NBR1 autophagy cargo receptor 1 gene, were upregulated and downregulated by both *ATP7B* KO and *ATP7B* KO + Cu, respectively. These genes were also included in the lncRNA-mRNA regulatory network and interacted with multiple DEGs, showing the involvement of autophagy in HLD.

This study identified that downregulated genes *EPO*, *IRS1*, and *PPARGC1A* were involved in biological processes related to chemical homeostasis, Jak-STAT signaling pathway, and adipocytokine signaling pathway. EPO plays key roles in bone, iron, Cu, and O_2 homeostasis (14, 15). The addition of EPO protein to rats with obstructive jaundice increased zinc levels in the serum and liver and decreased the levels of alanine aminotransferase, alkaline phosphatase, total bilirubin, and liver damage (16). Cu deficiency was involved in EPO-resistant anemia in hemodialysis patients, while Cu deficiency correction improved EPO unresponsiveness (17). EPO induced the tyrosine phosphorylation of IRS2 and then activated phosphatidylinositol 3-kinase (PI3K) (18). Supplements with exogenous EPO for four weeks stimulated the Jak2/STAT5/PI3K/Akt signal pathway and suppressed the overactivation of GSK-3β in the hippocampus (18). This study showed that *EPO* was downregulated in HepG2 cells with *ATP7B* KO and Cu treatments, and was involved in the Jak-STAT signaling pathway. EPO downregulation might play a crucial role in HLD pathogenesis via this pathway.

PPARGC1A is a master regulator of mitochondrial genes and its expression is decreased in type 2 diabetes (T2D) patients with a reduction in insulin secretion (20). *PPARGC1A* rs8192678 (Gly482Ser) was associated with the accumulation of subcutaneous adiposity and worsening insulin resistance, while *PPARGC1A* rs2970852 modified the effects of metformin on triacylglycerol levels (21). Both the deficiency and reduced expression of *IRSs* and *PPARGC1A* proteins were related to elevated oxidative stress and inflammation (22-24). Our present study showed that the *IRS1* and *PPARGC1A* genes were downregulated in the *ATP7B* KO cells with and without Cu toxicity. *EPO*, *IRS1*, and *PPARGC1A* genes were all targeted by four downregulated lncRNAs including *AFDN-DT*, *TOB1-AS1*, *DDN-AS1*, and *PCAT6*. EPO is an anti-apoptotic, anti-inflammatory, and angiogenetic cytokine that has protective properties against oxidative stress (16, 25, 26). However, none of these lncRNAs is associated with either

inflammation or oxidative stress. These data showed that the downregulation of these genes and lncRNAs in HLD play novel roles in HLD and may be responsible for Cu-induced oxidative stress. However, the strategies aiming at upregulating *EPO*, *IRS1*, or *PPARGC1A* genes may be potential therapeutic targets for HLD with mutations or deficiencies of them.

Other genes and lncRNAs in the two clusters including the upregulated genes *CLCF1* and *CCND3* and lncRNAs *MALAT1*, *LINC00324*, and *MIR22HG* may have novel roles in HLD. Genes *CLCF1* and *CCND3* are associated with the Jak/STAT signaling that relates to cell cycle and proliferation (27, 28). CLCF1 is a member of the IL-6 family and is also known as a neurotrophin 1 (29). CLCF1 interacts with the leukemia inhibitory factor β subunit (LIFR) or cytokine receptor-like factor 1 (CRLF1), which then stimulates the STAT3 and ERK1/2 signalings (29). However, our present study showed that the *LIFR* gene was downregulated, but the *CLCF1* gene was upregulated in *ATP7B* KO cells either with Cu toxicity or not. These results showed that the association of *CLCF1* with HLD may not be mediated by *CRLF1* and *LIFR*. The association of them with Cu accumulation and HLD pathogenesis or development should be investigated.

Most of the upregulated lncRNAs interacted with *CLCF1* and *CCND3*, including *MALAT1*, *LINC00324*, and *MIR22HG*, have shown proliferation and anti-proliferation effects in cancer cells or hepatocytes (30-33). *MALAT1* is elevated during liver regeneration and promotes hepatocyte proliferation by promoting *CCND*1 expression (33). *MALAT1* is upregulated in human hepatocytes under hypoxia/reoxygenation conditions, and its suppression was correlated with decreased inflammation induced by hypoxia/reoxygenation, showing that *MALAT1* expression might aggravate the liver injury (32). Altogether, these results provide a reference for the association of lncRNA-mediated cell proliferation and inflammation with HLD. However, further experiments should be performed to investigate the association of the DEGs and DElncRNAs with the development and pathogenesis of HLD.

Conclusion

The pathogenesis of HLD was associated with the reduced expression of genes including *EPO*, *IRS1*, and *PPARGC1A* and upregulated expression of genes including *CCND3*. DElncRNAs including downregulated *AFDN-DT* and *PCAT6* and upregulated *MALAT1* were correlated with those DEGs closely in HLD. These factors contributed to HLD via the signaling pathways including the Jak-STAT signaling pathway. This study pointed out the potential roles and importance of these genes in HLD pathogenesis. However, the verification of the above results should be performed. Therefore, more experiments are needed to be performed to verify the associations of them with HLD.

Journalism Ethical considerations

Ethical issues (Including plagiarism, informed consent, misconduct, data fabrication and/or falsification, double publication and/or submission, redundancy, etc.) have been completely observed by the authors.

Acknowledgements

Key Project of Natural Science Research Project of Universities in Anhui Province(KJ2021A0551); Research Fund of Anhui University of Chinese Medicine(2020sjzd05).

Conflict of Interest

The authors declare that there is no conflict of interest.

References

1. Squitti R, Siotto M, Arciello M, Rossi L (2016). Non-ceruloplasmin bound copper and ATP7B gene variants in Alzheimer's disease.

Metallomics, 8: 863-873.
2. Nishimuta M, Masui K, Yamamoto T, et al (2018). Copper deposition in oligodendroglial cells in an autopsied case of hepatolenticular degeneration. *Neuropathology,* 38(3): 321-328.
3. Ovchinnikov A, Shprakh V (2016). Hepatolenticular degeneration: diagnostic difficulties (practical experience). *Acta Biomedica Scientifica,* 1: 198-201.
4. Bandmann O, Weiss KH, Kaler SG (2015). Wilson's disease and other neurological copper disorders. *Lancet Neurol,* 14: 103-113.
5. Yang K, Deng Z, Wang J, Jiang L (2017). Clinical analysis of hepatolenticular degeneration in 38 children. *J Clin Pediatr,* 35: 733-736.
6. Polishchuk EV, Merolla A, Lichtmannegger J, et al (2019). Activation of autophagy, observed in liver tissues from patients with Wilson disease and from ATP7B-deficient animals, protects hepatocytes from copper-induced apoptosis. *Gastroenterology,* 156: 1173-1189. e1175.
7. Wu F, Wang J, Pu C, Qiao L, Jiang C (2015). Wilson's disease: a comprehensive review of the molecular mechanisms. *Int J Mol Sci,* 16: 6419-6431.
8. Robinson MD, McCarthy DJ, Smyth GK (2010). edgeR: a Bioconductor package for differential expression analysis of digital gene expression data. *Bioinformatics,* 26(1): 139-140.
9. Kumar L, Futschik ME (2007). Mfuzz: a software package for soft clustering of microarray data. *Bioinformation,* 2(1): 5-7.
10. Bao R, Huang L, Andrade J, et al (2014). Review of current methods, applications, and data management for the bioinformatics analysis of whole exome sequencing. *Cancer Inform,* 13(Suppl 2):67-82.
11. Tang B, Pan Z, Yin K, Khateeb A (2019). Recent advances of deep learning in bioinformatics and computational biology. *Front Genet,* 10: 214.
12. Yang F, Liao J, Pei R, et al (2018). Autophagy attenuates copper-induced mitochondrial dysfunction by regulating oxidative stress in chicken hepatocytes. *Chemosphere,* 204: 36-43.
13. Tsang T, Posimo JM, Gudiel AA, Cicchini M, Feldser DM, Brady DC (2020). Copper is an essential regulator of the autophagic kinases ULK1/2 to drive lung adenocarcinoma. *Nat Cell Biol,* 22: 412-424.
14. Singbrant S, Russell MR, Jovic T, et al (2011). Erythropoietin couples erythropoiesis, B-lymphopoiesis, and bone homeostasis within the bone marrow microenvironment. *Blood,* 117: 5631-5642.
15. Frýdlová J, Rychtarčíková Z, Gurieva I, Vokurka M, Truksa J, Krijt J (2017). Effect of erythropoietin administration on proteins participating in iron homeostasis in Tmprss6-mutated mask mice. *PLoS One,* 12: e0186844.
16. Aliosmanoglu I, Kapan M, Gul M, et al (2013). Effects of Erythropoietin on the Serum and Liver Tissue Levels of Copper and Zinc in Rats with Obstructive Jaundice. *J Med Biochem,* 32: 47-51.
17. Higuchi T, Matsukawa Y, Okada K, et al (2006). Correction of copper deficiency improves erythropoietin unresponsiveness in hemodialysis patients with anemia. *Intern Med,* 45(5): 271-273.
18. Verdier F, Chrétien S, Billat C, Gisselbrecht S, Lacombe C, Mayeux P (1997). Erythropoietin induces the tyrosine phosphorylation of insulin receptor substrate-2 an alternate pathway for erythropoietin-induced phosphatidylinositol 3-kinase activation. *J Biol Chem,* 272: 26173-26178.
19. Ma S, Chen J, Chen C, et al (2018). Erythropoietin rescues memory impairment in a rat model of chronic cerebral hypoperfusion via the EPO-R/JAK2/STAT5/PI3K/Akt/GSK-3β pathway. *Mol Neurobiol,* 55: 3290-3299.
20. Ling C, Del Guerra S, Lupi R, et al (2008). Epigenetic regulation of PPARGC1A in human type 2 diabetic islets and effect on insulin secretion. *Diabetologia,* 51: 615-622.
21. Franks PW, Christophi CA, Jablonski KA, et al (2014). Common variation at PPARGC1A/B and change in body composition and metabolic traits following preventive interventions: the Diabetes Prevention Program. *Diabetologia,* 57: 485-490.
22. Lin J, Handschin C, Spiegelman BM (2005). Metabolic control through the PGC-1 family of transcription coactivators. *Cell Metab,* 1: 361-370.
23. Pradhan AD, Manson JE, Rifai N, Buring JE, Ridker PM (2001). C-reactive protein, interleukin 6, and risk of developing type 2 diabetes mellitus. *JAMA,* 286: 327-334.
24. Fontecha-Barriuso M, Martín-Sánchez D, Martinez-Moreno JM, et al (2019). PGC-1α defi-

ciency causes spontaneous kidney inflammation and increases the severity of nephrotoxic AKI. *J Pathol,* 249: 65-78.

25. Sheldon RA, Windsor C, Lee BS, Cabeza OA, Ferriero DM (2017). Erythropoietin treatment exacerbates moderate injury after hypoxia-ischemia in neonatal superoxide dismutase transgenic mice. *Dev Neurosci,* 39: 228-237.
26. Zhang X, Dong S (2019). Protective effects of erythropoietin towards acute lung injuries in rats with sepsis and its related mechanisms. *Ann Clin Lab Sci,* 49: 257-264.
27. Steelman L, Pohnert S, Shelton J, Franklin R, Bertrand F, McCubrey J (2004). JAK/STAT, Raf/MEK/ERK, PI3K/Akt and BCR-ABL in cell cycle progression and leukemogenesis. *Leukemia,* 18: 189-218.
28. Fuke H, Shiraki K, Sugimoto K, et al (2007). Jak inhibitor induces S phase cell-cycle arrest and augments TRAIL-induced apoptosis in human hepatocellular carcinoma cells. *Biochem Biophys Res Commun,* 363: 738-744.
29. Sims NA (2015). Cardiotrophin-like cytokine factor 1 (CLCF1) and neuropoietin (NP) signalling and their roles in development, adulthood, cancer and degenerative disorders. *Cytokine Growth Factor Rev,* 26: 517-522.
30. Su W, Guo C, Wang L, et al (2019). LncRNA MIR22HG abrogation inhibits proliferation and induces apoptosis in esophageal adenocarcinoma cells via activation of the STAT3/c-Myc/FAK signaling. *Aging (Albany NY),* 11: 4587.
31. Gao J, Dai C, Yu X, Yin XB, Zhou F (2020). Long noncoding RNA LINC00324 exerts protumorigenic effects on liver cancer stem cells by upregulating fas ligand via PU box binding protein. *FASEB J,* 34: 5800-5817.
32. Zhang Y, Zhang H, Zhang Z, et al (2019). LncRNA MALAT1 cessation antagonizes hypoxia/reoxygenation injury in hepatocytes by inhibiting apoptosis and inflammation via the HMGB1-TLR4 axis. *Mol Immunol,* 112: 22-29.
33. Li C, Chang L, Chen Z, Liu Z, Wang Y, Ye Q (2017). The role of lncRNA MALAT1 in the regulation of hepatocyte proliferation during liver regeneration. *Int J Mol Med,* 39: 347-356.